[CANCER RESEARCH 64, 3599–3606, May 15, 2004]

Thioredoxin Is Downstream of Smad7 in a Pathway That Promotes Growth and Suppresses Cisplatin-Induced Apoptosis in Pancreatic Cancer

Nichole Boyer Arnold,[1] Knut Ketterer,[1] Jörg Kleeff,[2] Helmut Friess,[2] Markus W. Büchler,[2] and Murray Korc[1]

[1]Departments of Medicine and Pharmacology and Toxicology, Dartmouth Medical School, Hanover, New Hampshire, and [2]Department of General Surgery, University of Heidelberg, Heidelberg, Germany

ABSTRACT

Pancreatic ductal adenocarcinoma (PDAC) is an aggressive human malignancy in which Smad7 is commonly overexpressed. Analysis by differential display identified thioredoxin-1 (*TRX*) as a gene whose basal expression is increased in COLO-357 pancreatic cancer cells engineered to overexpress Smad7. To delineate the biological consequences of TRX overexpression, we assessed TRX mRNA levels in PDAC and studied the effects of increased TRX levels in Smad7-overexpressing cells. By northern blotting, TRX mRNA levels were increased in PDAC samples by comparison with the normal pancreas. Moreover, analysis of laser-captured pancreatic cancer cells revealed parallel increases in Smad7 and TRX mRNA levels. Retroviral infection of an antisense TRX cDNA suppressed TRX protein levels and blunted the increased capacity of Smad7-overexpressing cells to form colonies in soft agar. 1-Methyl-propyl-2-imidazolozyl disulfide, a TRX inhibitor, markedly suppressed the growth of sham-transfected COLO-357 cells and enhanced the growth inhibitory actions of *cis*-diamminedichloroplatinum(II) (CDDP). CDDP also induced apoptosis, as evidenced by induction of DNA laddering, PARP cleavage, and caspase-3/9 activities. These pro-apoptotic actions were greatly attenuated in Smad7-overexpressing cells, which exhibited a more prolonged association of TRX with the apoptosis inducer apoptosis signal-regulating kinase-1, and enhanced nuclear factor κB activation in response to CDDP. These findings suggest that TRX is downstream of Smad7 in a pathway that confers a growth advantage to pancreatic cancer cells and that increases their resistance to CDDP-mediated apoptosis, implying novel regulatory functions for Smad7.

INTRODUCTION

The transforming growth factor-β (TGF-β) superfamily of cytokines inhibits the growth of many epithelial cell types. TGF-β inhibitory effects are mediated via heteromeric complex formation of TGF-β type II and type I serine/threonine kinase receptors (TβRI and TβRII). Upon TGF-β1 ligand binding to TβRII, TβRII phosphorylates serine and threonine residues within the GS domain of TβRI, which activates its kinase activity. TβRI then phosphorylates the receptor-regulated Smads (R-Smads) Smad2 and Smad3. Activated Smad2/3 form a complex with Smad4 (Co-Smad), and translocate to the nucleus to act as transcriptional modulators of TGF-β1-regulated genes (1). Another class of Smads, the inhibitory Smads, Smad6 and Smad7, inhibit TGF-β1 signaling by binding Smad4 to prevent association with Smad2/3 (Smad6) or by binding to TβRI and preventing phosphorylation of Smad2 and Smad3 (Smad7; Refs. 2, 3).

In addition to inhibiting TGF-β1 signaling, Smad7 may function as a TGF-β1-independent transcriptional modulator. The Smad7 MH2 domain, when fused to a DNA-binding domain acts as a potential transcriptional activator (4). Furthermore, when Smad7 is complexed to the DNA-binding domain of GAL4, it increases the transcription of a minimal retinoid acid receptor-β2 GAL4-TGTA luciferase construct (5). Smad7 also associates with transcriptional repressor histone deacetylase-1 (6), and the transcriptional coactivators p300 (7) and yes-associated protein (YAP65; Ref. 8). Thus, Smad7 may exert coactivator/corepressor functions depending on the cellular context in which it is expressed.

Thioredoxin-1 (TRX), along with thioredoxin reductase and NADPH, make up the thioredoxin redox system (9). TRX contains a conserved catalytic site (-Trp-Cys-Gly-Pro-Cys- Lys) with an active selenocysteine residue that serves as a hydrogen donor for oxidation-reduction (redox) reactions and is involved in the reduction of crucial disulfide bonds that determine the protein conformation and DNA-binding ability of the transcription factors AP-1 (Jun/Fos), nuclear factor κB (NFκB), and p53 (10). Overexpression of TRX in MCF-7 breast cancer cells stimulates their anchorage-independent growth and enhances their tumorigenicity (11). Furthermore, TRX expression is increased in multiple human cancers such as lung, colon, gastric, and liver carcinomas; adult T cell leukemia; and testicular cancer (9). Together, these observations suggest that TRX may have an important role in modulating cancer growth.

Pancreatic ductal carcinoma (PDAC) is a deadly disease that is characterized by enhanced cellular proliferation, resistance to apoptosis and chemotherapeutic agents, aberrant activation of tyrosine kinase-dependent signaling pathways, and perturbations in TGF-β signaling pathways (12). Resistance to TGF-β-mediated growth inhibition occurs as a consequence of Smad4 mutations, Smad7 overexpression, or TβRI underexpression (13–15). COLO-357 pancreatic cancer cells have wild-type Smad4, express normal levels of TβRI and TβRII, and are growth inhibited by TGF-β1 (16). When engineered to overexpress Smad7 (CS7 cells), these cells become resistant to TGF-β1-mediated growth inhibition and exhibit enhanced anchorage-independent growth and enhanced tumorigenicity in nude mice (14). In the present study, we used the technique of differential display to assess whether increased Smad7 expression in CS7 cells is associated with an altered gene expression profile and identified TRX as an abundant mRNA in these cells. Using laser-capture micro-dissection and quantitative PCR, we found parallel increases in TRX and Smad7 mRNA levels in 50% of tested PDAC samples. To assess the biological significance of TRX overexpression, we used an antisense strategy to suppress TRX expression in CS7 clones and the TRX inhibitor 1-methyl-propyl-2-imidazolozyl disulfide (PX-12) to inhibit TRX activity. Suppression of TRX expression in CS7 clones attenuated the Smad7-induced increase in anchorage-independent growth. Furthermore, inhibition of TRX activity by PX-12 inhibited cell growth, and this growth-suppressive effect was blunted in CS7 clones. *cis*-Diamminedichloroplatinum(II) (CDDP)-mediated activation of apoptosis was also greatly attenuated in CS7 clones, which, in contrast to Sham cells, exhibited NFκB activation in conjunction with enhanced degradation of inhibitor of nuclear factor-κB α (IκB-α). These findings suggest that TRX is downstream of Smad7 in a pathway that may act to promote growth and induce apoptosis resistance in pancreatic cancer cells.

Received 9/23/03; revised 2/4/04; accepted 2/26/04.

Grant support: United States Public Health Service Grant CA-75059 (M. Korc) and University of California at Irvine Cancer Research Institute Grant NCI 5 T32 CA09054 (N. Arnold). N. Arnold was the recipient of a graduate training award from the Training Program in Carcinogenesis and a postdoctoral fellowship award from the George E. Hewitt Foundation for Medical Research.

The costs of publication of this article were defrayed in part by the payment of page charges. This article must therefore be hereby marked *advertisement* in accordance with 18 U.S.C. Section 1734 solely to indicate this fact.

Requests for reprints: Murray Korc, 1 Medical Center Drive, Dartmouth-Hitchcock Medical Center Lebanon, NH 03755. Phone: (603) 650-7936; Fax: (603) 650-6122; E-mail: murray.korc@dartmouth.edu.

MATERIALS AND METHODS

Reagents and Cell Culture. COLO-357 human pancreatic cancer cells were grown in. DMEM supplemented with 10% fetal bovine serum, 100 units/ml penicillin, and 100 μg/ml streptomycin (all from Irvine Scientific, Irvine, CA) in 5% CO_2 (17). Sham- and Smad7-transfected cells were grown in the presence of 400 μg/ml G418 (Invitrogen, Carlsbad, CA). For differential display and northern blotting, cells (70% confluent) were incubated in serum-free medium (0.1% BSA, 5 μg/ml apoptransferrin, 5 ng/ml sodium selenite, and antibiotics) for 24 h before TGF-β1 (Genentech, Inc., South San Francisco, CA) addition. CDDP and pyrrolidine dithiocarbamate were purchased from Sigma. PX-12 was a gift from ProLX Pharmaceuticals. SN50 and SN50M were purchased from BioMol (Plymouth Meeting, PA).

Differential Display. The technique of differential display was performed according to the GenHunter protocol with some modifications (18). RNA (100 μg) was treated with RNase-free DNase from Roche (Indianapolis, IN) in the presence of RNasin RNase inhibitor. RNA was reverse transcribed to cDNA with Superscript II from Invitrogen using an anchored ($HT_{11}A$) primer. The cDNA was PCR amplified in the presence of [^{33}P]dCTP in duplicate using the anchored primer and multiple arbitrary primers as specified in the GenHunter kit (Nashville, TN). PCR products were separated on an 8% denaturing polyacrylamide gel, exposed to Kodak Biomax, excised, and eluted from the gel. Desired PCR products were then amplified using the same set of primers from the initial differential display, TA subcloned (Invitrogen), and sequenced on an ABI sequencer (University of California-Irvine DNA Core Facility). Genes were then identified by BLAST of the GenBank Database.

Northern Blot Analysis. Total RNA was extracted, size fractioned, transferred onto nylon membranes, and UV cross-linked, as reported previously (19). Blots were hybridized overnight with the [^{32}P]dCTP-labeled differential display TRX cDNA probe, washed extensively, and then exposed at −80°C to Kodak Biomax MS film with intensifying screens. A 190-bp 7S cDNA probe was used to confirm equal RNA loading and transfer. Normal pancreatic tissues and PDAC samples were obtained through an organ donor program and from pancreatic cancer patients undergoing surgery at the University of Heidelberg (Germany). All studies were approved by the Ethics Committee of the University of Heidelberg and by the Human Subjects Committees at the University of California, Irvine, and Dartmouth Medical School, Hanover.

Immunoblotting and Immunoprecipitation Studies. For TRX immunoblotting, cells were washed, lysed in the presence of protease inhibitors, subjected to 15% SDS-PAGE, and transferred to nitrocellulose membranes (10 μg/lane) as reported previously (19). Membranes were incubated at 23°C for 1 h with 0.1 μg/ml of a highly specific mouse antihuman TRX antibody (Serotec, Raleigh, NC), washed, and incubated with goat antimouse secondary antibody. Bound antibody was visualized using enhanced chemiluminescence (Pierce, Rockford, IL). The membranes were then stripped and probed with an anti-ERK2 antibody (Santa Cruz Biotechnology, Santa Cruz, CA). Cell lysates were also subjected to 9% SDS-PAGE gels and probed for IκB-α and ASK1 (Santa Cruz Biotechnology), and phospho-p38 and phospho-JNK (Promega, Madison, WI). For immunoprecipitation experiments, cell lysates (0.5 mg) were immunoprecipitated with the TRX antibody (2 μg), and the resulting complex was bound with protein AG-Sepharose beads, washed, and subjected to SDS-PAGE and immunoblotting for ASK1 analysis.

Soft Agar Assay. A full-length thioredoxin cDNA, cloned in the antisense direction in the retroviral expression vector pLNCX, was transfected by the LipofectAMINE (Invitrogen) method into PT67 cells, which are competent to replicate retroviral particles. Stable clones were selected and expanded in G418 selection medium. Smad7-overexpressing cells were infected at a multiplicity of infection of 300 for 24 h, allowed to recover overnight, and re-infected for an additional 24 h. Basal anchorage-independent cell growth was assessed by a double-layer soft agar assay (14). Sham and CS73 cells were infected with retrovirus containing either an empty vector or a full-length antisense thioredoxin cDNA. Cells (8×10^3) were suspended in complete medium containing 0.3% agar and seeded in triplicate in 6-well plates onto a base layer of complete medium containing 0.5% agar. Complete medium containing 0.3% agar was added every 5 days for 15 days, before colony counting.

Growth Assay. The MTT [3-(4,5-methylthiazol-2-yl)-2,5-diphenyl-tetrazolium bromide] growth assay is a modification of the assay developed by Mosmann (20), and we have shown previously that in pancreatic cancer cells, the results of the MTT assay correlate well with results obtained by cell counting with a hemocytometer and by monitoring [^{3}H]thymidine incorporation (21, 22). The assay relies on the uptake and metabolism of the tetrazolium salt (MTT), and only viable cells take up and metabolize the compound into dark blue formazon crystals. Cells were plated at a density of 8,000 cells/well in 96-well microtiter plates (Costar) and allowed to adhere overnight. Cells were then treated for 24 h. After incubation, 62.5 μg/well MTT solution was added for 4 h. The medium was then aspirated, and 100 μl of acidified isopropanol (0.04 N) were added followed by vigorous shaking on a platform shaker to lyse the cells. Colorimetric change was read on a Microtiter plate reader with a 570-nm filter.

Laser Capture Microdissection and Real-Time Quantitative PCR. Cancer cells from 5–10-μM sections of frozen PDAC samples were microdissected using an Arcturus Laser Capture Microdissecting system (23). RNA from captured cells was extracted using the SV Total RNA Extraction kit (Promega). RNA (5 ng/sample) was reverse transcribed using the Sensiscript cDNA Amplification kit (Qiagen, Valencia, CA). Real-time fluorescent TaqMan PCR (ABI Prism 7700 Sequence Detection system; Applied Biosystems) was performed as reported previously (19), using primers and probes specific for human thioredoxin and Smad7. β-Actin was used as a reference gene to control RNA input and for efficiency of reverse transcription. The following cycling conditions were used: 50°C for 2 min and 95°C for 10 min; followed by 40 cycles at 95°C for 15 s and 60°C for 1 min.

DNA Laddering. For nonradioactive DNA laddering detection, DNA from treated and untreated cells was isolated in DNA extraction buffer (50 mM Tris-Cl, 0.05% SDS, 0.1% TX-100, 50 μg/ml RNase A, 50 μg/ml proteinase K, and 25 mM EDTA), phenol/chloroform extracted, and ethanol-precipitated. DNA (1 μg) was then size-fractionated on 1.2% agarose gels containing ethidium bromide (0.1 μg/ml) and visualized by UV transillumination.

Poly(ADP-Ribose) Polymerase (PARP) Cleavage. Cells were lysed in the presence of protease inhibitors, subjected to 7.5% SDS-PAGE (25 μg/lane), and transferred to nitrocellulose membranes as reported previously (19). Membranes were incubated at 23°C for 1 h with 1 μg/ml of a highly specific (SA-250) mouse anti-PARP antibody (BioMol) washed, and incubated with goat antimouse secondary antibody. Bound antibody was visualized using enhanced chemiluminescence from Pierce.

Measurement of Caspase Activity. Caspase-3 and caspase-9 activities were measured using Colorimetric Assay kits from R&D Systems (Minneapolis, MN). In brief, cells were scraped into PBS, pelleted at low speed, and resuspended in lysis buffer for 10 min at 4°C. Cell lysates were cleared by centrifugation and assayed for caspase-3 and caspase-9 activity using DEVD-pNA and LEHD-pNA peptide substrates, respectively, and incubated for 6 h at 37°C. The activities were quantified spectrophotometrically at a wavelength of 405 nm. Caspase activity was calculated as the change in absorbance at 405 nm and divided by total protein concentration.

Luciferase Assay. Cells were plated in 12-well plates at a density of 40,000 cells/well and allowed to adhere overnight. Transfections consisting of a PathDetect pNFκB-Luciferase (Stratagene, San Diego, CA) construct (0.5 μg) containing five copies of the NFκB response element and 0.25 μg of CMV-β-galactosidase plasmid were incubated with 0.75 μg of Nupherin Neuron (BioMol) for 30 min at 25°C. The resulting complexes were then incubated with LipofectAMINE (Invitrogen) according to the manufacturer's instructions. Cells were then transfected for 12 h and allowed to recover overnight in complete medium before treatments. Relative luciferase activity was calculated by dividing the luciferase values by the β-galactosidase values.

Electrophoretic Mobility Shift Analysis. Nuclear extracts were prepared according to a modified Dignam *et al.* (24) protocol. In brief, cells were scraped in PBS containing protease inhibitors (1 mM $NaVO_3$; 1 μg/ml leupeptin, pepstatin, and aprotonin; and 1 mM phenylmethylsulfonyl fluoride), pelleted, and resuspended in hypotonic buffer A [10 mM 4-(2-hydroxyethyl)-1-piperazineethanesulfonic acid (pH 7.5), 10 mM KCl, 1 mM EDTA, 1 mM EGTA, 0.5 mM DTT, and protease inhibitors] and allowed to swell for 10 min on ice. NP40 was added to a final concentration of 0.5%, and cells were incubated on ice for 10 min before centrifugation for 2 min at 10,000 rpm. The supernatant was removed, and nuclei were resuspended in high-salt buffer C [20 mM 4-(2-hydroxyethyl)-1-piperazineethanesulfonic acid (pH 7.5), 0.4 M NaCl, 1 mM EDTA, 1 mM EGTA, and protease inhibitors] and incubated with gentle shaking for 15 min on ice before centrifugation at 10,000 rpm for 2 min. Electrophoretic mobility shift analysis reactions were performed with 5 μg of nuclear extracts and 50,000 cpm of a ^{32}P-labeled NFκB consensus oligonucleotide (Santa Cruz Biotechnology). Binding reactions were carried out at

23°C for 30 min. Samples were analyzed for protein/DNA complex formation on a 5% nondenaturing polyacrylamide. The gel was then dried and exposed to Kodak Biomax film.

Intracellular Reactive Oxygen Species (ROS) Measurement. Measurement of ROS by CDDP was determined using CMH_2DCFDA (Molecular Probes, Eugene, OR; 25) and fluorescence measured at 480 nM using a fluorescence plate reader.

RESULTS

Sham-transfected (Sham) and Smad7-overexpressing COLO-357 cells (CS7) were serum starved for 24 h and then incubated with 1 nM TGF-β1 for 24 h. The extracted RNA was subjected to differential display analysis, revealing increased TRX expression in untreated and TGF-β1-treated Smad7-overexpressing cells (data not shown). Northern blotting of RNA from Sham cells and three CS7 clones confirmed markedly increased basal levels of TRX mRNA in all three clones by comparison with Sham cells (Fig. 1*A*).

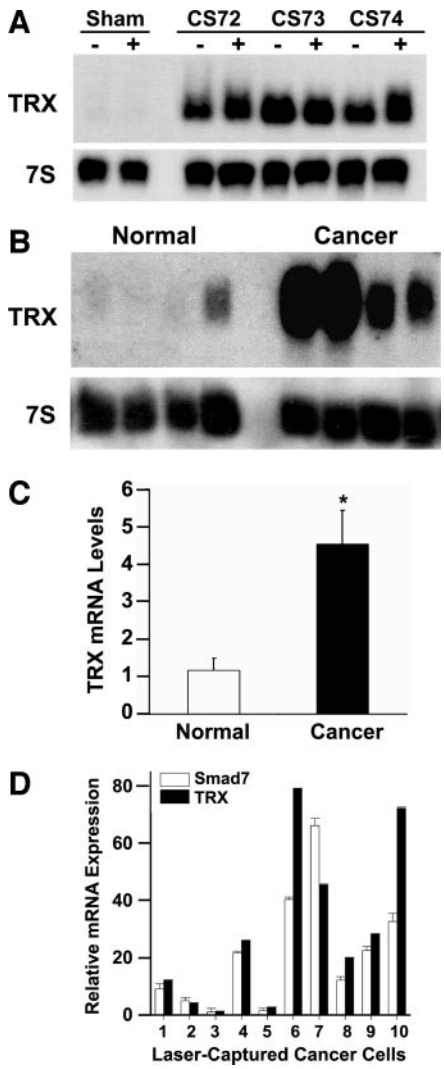

Fig. 1. Thioredoxin expression in COLO-357 and PDAC. *A*, total RNA (20 μg/lane) isolated from the indicated cells in the absence (control) or presence of 1 nM TGF-β1 were subjected to Northern blot analysis using a [^{32}P]dCTP-labeled 150-bp thioredoxin cDNA obtained from differential display (1,000,000 cpm/ml). A 7S cDNA probe (50,000 cpm/ml) was used as loading control. Exposure times for thioredoxin were 4 days for COLO-357, 4 h for CS73, and 5 h for 7S. *B*, Northern blot analysis of PDAC tissue. Total RNA (10 μg/lane) from normal and pancreatic cancer tissue was subjected to Northern blot analysis using a thioredoxin cDNA probe. A 7S cDNA probe was used as a loading and transfer control. *C*, densitometric analysis. Thioredoxin mRNA levels from 18 normal and 23 cancer samples were quantified by densitometry and normalized to the 7S signal. Data are presented as the means ± SE. *, $P < 0.002$ by comparison with values in the normal pancreas. *D*, analysis of laser-captured samples. Smad7 and thioredoxin mRNA levels in laser-captured pancreatic cancer cells were quantified by TaqMan real-time quantitative PCR as described in "Materials and Methods." Results from triplicate reactions were normalized to a β-actin endogenous control for RNA input and are expressed as the means ± SD for thioredoxin and Smad7 RNA levels for each pancreatic cancer sample.

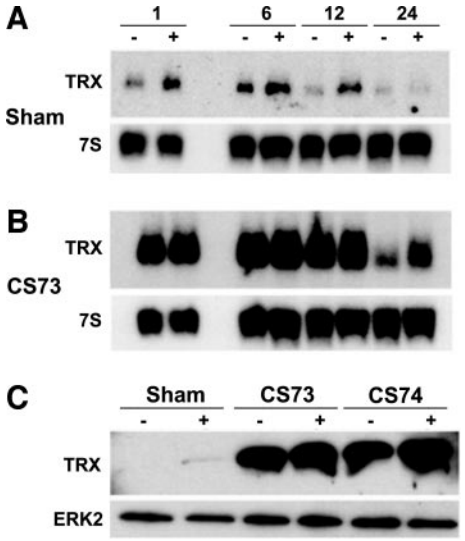

Fig. 2. Effects of TGF-β1 on TRX Levels. *A*, TGF-β1 time course and Northern blot analysis. Sham cells and a CS7 clone were serum starved for 24 h and then treated with TGF-β1 for 1, 6, 12, or 24 h. Total RNA (20 μg/lane) was hybridized as detailed in the legend to Fig. 1. Autoradiograms were exposed for 4 h (CS7–3) or 4 days (Sham). *B*, immunoblotting. Total cell lysates (10 μg/lane) from untreated (control) or TGF-β1-treated cells were subjected to 15% SDS-PAGE, transferred to an Immobilon-P membrane, and probed with a highly specific antithioredoxin antibody (100 ng/ml). Immunoblotting of the same filters with anti-ERK2 antibody (200 ng/ml) served to assess protein loading.

TRX expression is increased in multiple human cancers such as lung, colon, gastric, and liver carcinomas; adult T cell leukemia; and testicular cancer (9). To determine whether TRX mRNA levels are increased in PDAC, total RNA from normal and PDAC samples was analyzed by Northern blottting (Fig. 1*B*). Densitometric analysis from 18 normal and 23 PDAC samples revealed an approximately 4-fold increase in TRX mRNA levels in PDACs when compared with the normal pancreas (Fig. 1*C*). To assess whether there was a correlation between TRX and Smad7 mRNA levels in the same cancer cells in PDAC, RNA extracted from laser microdissected cancer cells was subjected to TaqMan real-time quantitative-PCR. There was a remarkable concordance between TRX and Smad7 mRNA levels in each sample (Fig. 1*D*), raising the possibility that Smad7 overexpression in PDAC contributes to the up-regulation of TRX.

Next, we sought to determine whether TGF-β1 modulated TRX expression and whether this effect was altered in the presence of high levels of Smad7. In the absence of TGF-β1, TRX mRNA levels in Sham cells were relatively low (4 d exposure of autoradiograph) but increased between 1 and 6 h and declined thereafter (Fig. 2*A*). By the end of the 24-h period, TRX mRNA levels were almost undetectable in Sham cells. In contrast, TRX mRNA levels were markedly elevated in the Smad7-overexpressing clone (4 h exposure of autoradiograph) at 1, 6, and 12 h and exhibited a slight decrease at 24 h, which was attenuated in the presence of TGF-β1 (Fig. 2*B*). The increase in TRX mRNA levels correlated well with increased TRX protein levels (Fig. 2*C*), and similar results were observed in two other clones (not shown).

Overexpression of TRX in MCF-7 cells has been shown previously to stimulate anchorage-independent growth and increase tumorigenicity (11). In the present study, CS7 cells exhibited increased (160 ± 8%) anchorage-independent growth by comparison with Sham cells. To determine whether TRX contributed to the increased anchorage-independent growth of CS7 cells, infection with a retroviral

vector containing a full-length antisense TRX cDNA was performed to suppress TRX protein levels (Fig. 3*B*). These cells exhibited an attenuated increase in colony formation (39 ± 2.3%) when compared with infection with empty vector (Fig. 3*A*), indicating that TRX overexpression in the Smad7-overexpressing cells contributes to increased anchorage-independent growth.

Inhibition of TRX activity by imidazolozyl disulfide compounds blocks cell cycle progression in MCF-7 cancer cells (26). Therefore, we next sought to determine the effects of TRX inhibition on the proliferation of Sham and CS7 cells. Accordingly, cells were incubated with increasing concentrations of PX-12. After 24 h, PX-12 (10 μM) attenuated the proliferation of Sham and CS7 cells by 85% and 45–65%, respectively (Fig. 4*A*).

Pancreatic cancer cells are resistant to apoptosis and are relatively insensitive to CDDP treatment but undergo apoptosis at high CDDP concentrations (27, 28). Moreover, TRX protects cells from oxidative stress-induced apoptosis by ROS (29) and from CDDP-mediated cytotoxicity (9, 30), whereas inhibition of TRX activity induces apoptosis in WEHI7.2 thymoma and HeLa cells (31, 32). Therefore, we next sought to characterize the effects of CDDP on cell growth and on apoptosis. CDDP (50 μM) markedly suppressed the proliferation of Sham cells by 64% but only inhibited the growth of CS7 clones by 25–30% (Fig. 4*B*). Cotreatment with PX-12 (10 μM) additively exerted a suppressive effect on cell growth in both the Sham and CS7 cells, which was again less effective in the CS7 cells (Fig. 4*B*). CDDP (50 μM) also induced apoptosis in Sham cells, as evidenced by DNA laddering (Fig. 5*A*) and PARP cleavage (Fig. 5*B*) and by the generation of high levels of caspase-3 and caspase-9 activity (Fig. 5, *C* and *D*). By contrast, under the same incubation conditions, CDDP failed to induce DNA laddering, PARP cleavage, or caspase-9 activities in CS7 cells (Fig. 5). Furthermore, the induction of caspase-3 activity in these cells was markedly attenuated (Fig. 5*C*).

In addition to stimulating cell proliferation and inhibiting apoptosis, TRX has been implicated in regulating the activity of the NFκB cell survival pathway (33). We therefore sought to determine whether the attenuated effect of CDDP in CS7 cells was due to enhanced NFκB activation. CDDP (50 μM) caused a marked increase in NFκB luciferase activity (2.2–3.0-fold) in CS7 cells but did not alter NFκB luciferase activity in Sham cells (Fig. 6*A*). The NFκB inhibitor pyrrolidine dithiocarbamate decreased basal NFκB activity and blocked the CDDP-mediated increase in NFκB activity (Fig. 6*A*). Furthermore, by electrophoretic mobility shift analysis, binding of NFκB was greatly increased by CDDP in CS7 cells but not in Sham cells (Fig. 6*B*).

To further characterize the mechanism whereby CDDP activated NFκB, we next examined the effects of CDDP on its major endogenous inhibitor, IκB-α. In Sham cells, 16 h after addition of CDDP (50 cM), there was only a slight decrease in IκB-α protein levels (Fig. 7*A*). By contrast, CDDP treatment of CS7 cells for 16 h was associated with a marked decrease in IκB-α levels in these cells, and this effect persisted for the next 8 h (Fig. 7*B*).

To determine whether suppression of NFκB activity could restore the ability of CDDP to activate pro-apoptotic pathways, we next examined the effects of a highly specific inhibitor of NFκB, SN50, on CDDP-mediated PARP cleavage. As in previous experiments, CDDP (50 μM) addition to Sham cells for 24 h induced PARP cleavage, but this effect was not observed in CS7 cells (Fig. 7*C*). SN50 at a concentration of 50 μM restored the ability of CDDP to induce PARP cleavage in CS7 cells (Fig. 7*C*). By contrast, a mutant and inactive form of SN50, SN50M, was ineffective in this regard (Fig. 7*C*).

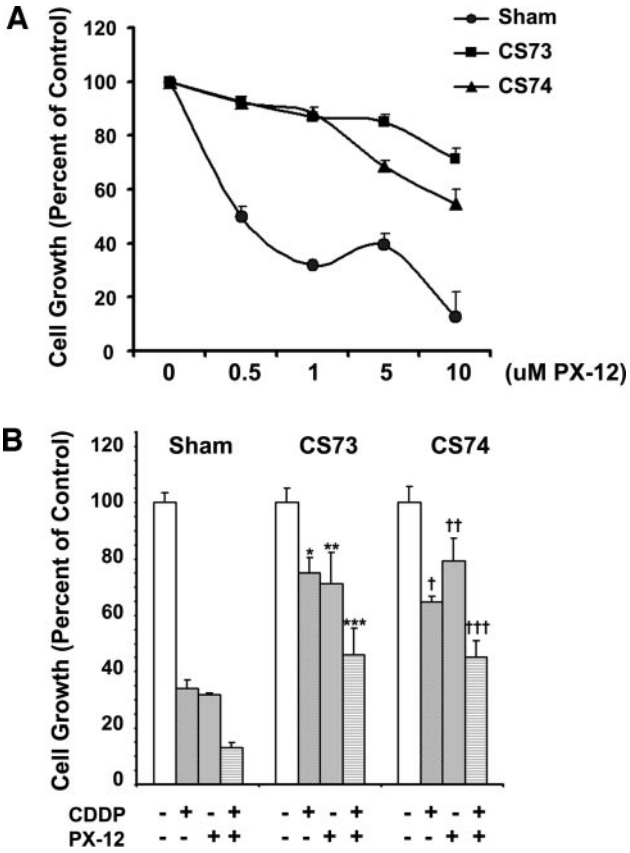

Fig. 4. Effects of PX-12 and CDDP on proliferation. *A*, Sham cells and Smad7 clones were plated at a density of 8,000 cells/well on 96-well microtiter plates and allowed to adhere overnight. Cells were then treated for 24 h with increasing concentrations of PX-12 (0–10 μM). Growth was assessed by the change in absorbance at 570 nM as described in "Materials and Methods." Data are presented as the means ± SE from three separate experiments *B*, cells were incubated for 24 h in the absence (−) or presence (+) of 10 μM PX-12 and/or 50 μM CDDP before the addition of MTT solution. Data are presented as the means ± SE of triplicate determinations per experiment from three individual experiments. *, $P < 0.03$; **, $P < 0.06$; and ***, $P < 0.07$ for CS73. †, $P < 0.01$; ††, $P < 0.02$; and †††, $P < 0.03$ for CS74 by comparison with corresponding values for Sham cells.

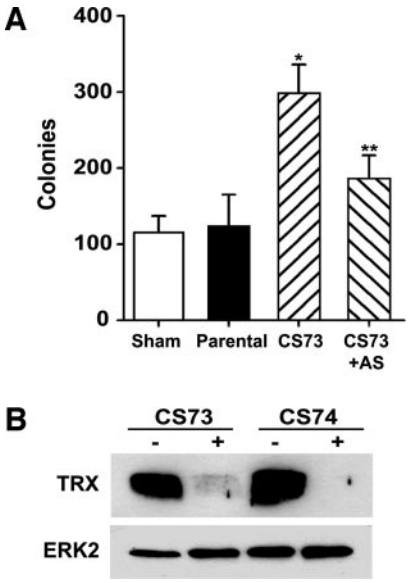

Fig. 3. Thioredoxin antisense expression and anchorage-independent cell growth. *A*, Colony formation in soft agar. Anchorage-independent growth of parental cells, Sham cells, CS73 cells, and CS73 cells infected with thioredoxin antisense was determined after 15 days. Data are presented as the means ± SE of triplicate determinations per experiment from three individual experiments. *, $P < 0.012$ when compared with values observed in Sham or parental cells; **, $P < 0.008$ when compared with values observed in CS73 vector control. *B*, immunoblotting. Cell lysates were harvested after infection with a retroviral thioredoxin antisense cDNA or empty vector and subjected to SDS-PAGE. Membranes were probed with a highly specific thioredoxin antibody.

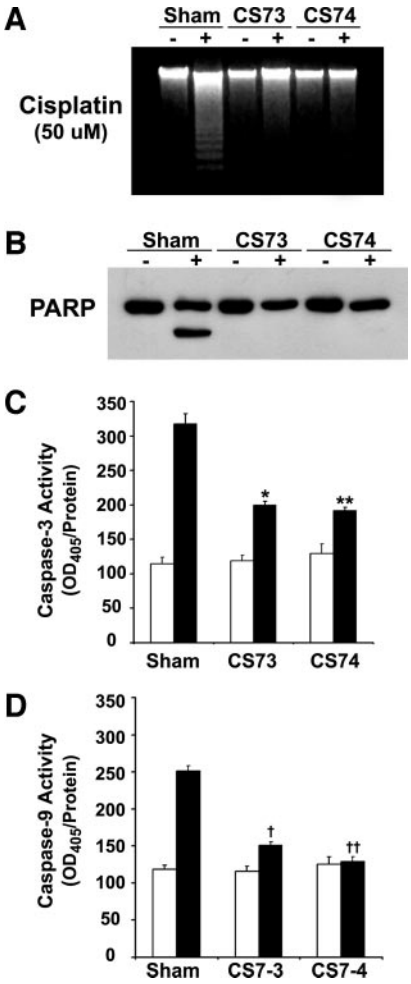

Fig. 5. DNA laddering, PARP cleavage, and caspase activation. *A*, Sham cells and Smad7 clones were treated with 50 μM CDDP for 24 h, and DNA (2 μg/lane) was run on a 1.2% agarose gel and stained with ethidium bromide as described in "Materials and Methods." *B*, Sham cells and Smad7 clones were treated for 24 h with 50 μM CDDP, and protein was extracted and subjected to Western blot analysis using an antibody that recognizes uncleaved and cleaved PARP. *C* and *D*, after 24 h of treatment with 50 μM CDDP, cell lysates were assayed for caspase-3 (*C*) and caspase-9 (*D*) activity. Total caspase activity was determined by dividing the change in absorbance at 405 nM by protein input. Data in *C* and *D* are the means ± SE of triplicate determinations per experiment from three individual experiments. *, $P < 0.06$; **, $P < 0.05$; †, $P < 0.05$; and ††, $P < 0.06$ by comparison with corresponding values in Sham cells.

Apoptosis signal-regulating kinase-1 (ASK1) is a multifunctional mitogen-activated protein (MAP) kinase kinase kinase member that induces apoptosis though activation of c-jun N-terminal kinase (JNK) and p38 MAP kinase (34). Its kinase activity is activated by various stress stimuli, including chemotherapeutic agents such as CDDP (35). TRX binds to ASK1, and the resulting protein-protein complex is devoid of ASK1 kinase activity (36). Therefore, we next sought to determine whether ASK1 levels were similar in Sham and CS7 cells and whether TRX associated with ASK1 in these cells. Immunoblotting with anti-ASK1 antibodies revealed that ASK1 protein levels were reduced by approximately 50% in CS7 cells by comparison with Sham cells (Fig. 8*A*). Moreover, TRX immunoprecipitation followed by immunoblotting for ASK1 revealed that TRX associated with ASK1 in both groups of cells (Fig. 8*B*). However, after a 24-h incubation period, CDDP decreased the amount of ASK1 that co-immunoprecipitated with TRX, and this effect was greater in Sham cells by comparison with the CS7 cells (Fig. 8*B*).

We next sought to determine whether there was differential activation of JNK and p38 MAP kinase in Sham and CS7 cells. Activation of p38 MAP kinase and JNK, determined using phosphospecific anti-p38 and anti-JNK antibodies, was evident at 16 and 6 h, respectively, after addition of CDDP (50 μM) in Sham cells, with the effects persisting for at least 24 h (Fig. 9*A*). By contrast, in CS7 cells, these effects were delayed and attenuated, with activation of p38 MAP kinase and JNK becoming evident only after 18 and 16 h, respectively (Fig. 9*B*).

ROS can increase the phosphorylation of p38 MAP kinase and JNK, thereby inducing apoptosis (37, 38). Furthermore, CDDP may increase ROS generation in certain cell types. Therefore, we next examined the effects of CDDP on ROS levels. However, CDDP (50 μM) did not significantly alter ROS levels in either Sham or CS7 cells (data not shown).

DISCUSSION

TGF-βs are multifunctional growth factors that inhibit the growth of epithelial cells, enhance the growth of mesenchymal cells, modulate components of the extracellular matrix, contribute to epithelial-mesenchymal transformation, suppress cancer directed immune mechanisms, and promote angiogenesis (39). TGF-βs often fail to suppress the growth of epithelial cell-derived cancers because these cells have acquired resistance to TGF-β-mediated growth inhibition. Such resistance may arise as a consequence of several different types of alterations. These include Smad4 mutations (40), overexpression of inhibitory Smad6 and Smad7 (14, 41), mutations in and/or decreased expression of *TβRI* or *TβRII* genes (42–44), structural or functional abnormalities in the p53 tumor suppressor gene (45), decreased ability to reduce the phosphorylation of the retinoblastoma gene product RB (46), and overexpression of H-*ras* (47), which induces TβRII down-regulation (48). In some cell types, TGF-βs may also act by activating *ras*-dependent pathways, as evidenced by the observation that expression of a dominant-negative N-*ras* construct partially attenuates the

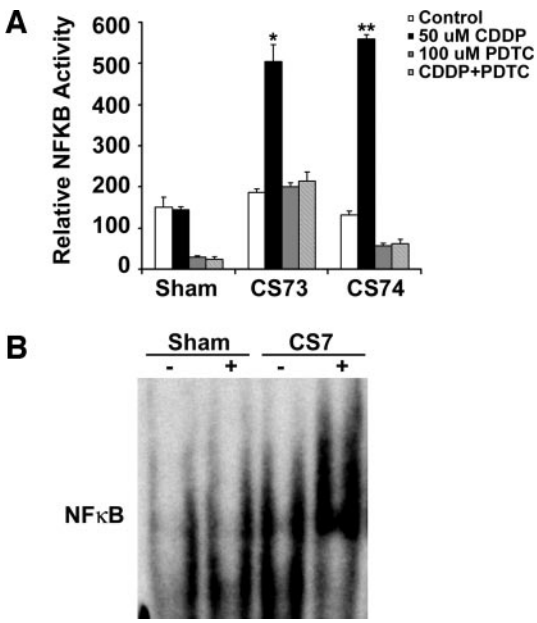

Fig. 6. NFκB activation by CDDP. *A*, Sham and Smad7 cells were plated to 12-well plates and transiently transfected as described in "Materials and Methods." Cells were transfected for 12 h and allowed to recover overnight in complete medium before treatment with 50 μM CDDP, 100 μM pyrrolidine dithiocarbamate, or both for 6 h. Relative luciferase activity was then calculated by dividing the luciferase values by the β-galactosidase values. Data are the means ± SE of triplicate determinations per experiment from three individual experiments. *, $P < 0.004$; **, $P < 0.001$ by comparison with corresponding values in Sham cells. *B*, Nuclear extracts from CDDP-treated Sham cells and a CS7 clone were incubated with 50,000 cpm of a ^{32}P-labeled NFκB consensus oligonucleotide (Santa Cruz Biotechnology) and subjected to electrophoretic mobility shift analysis.

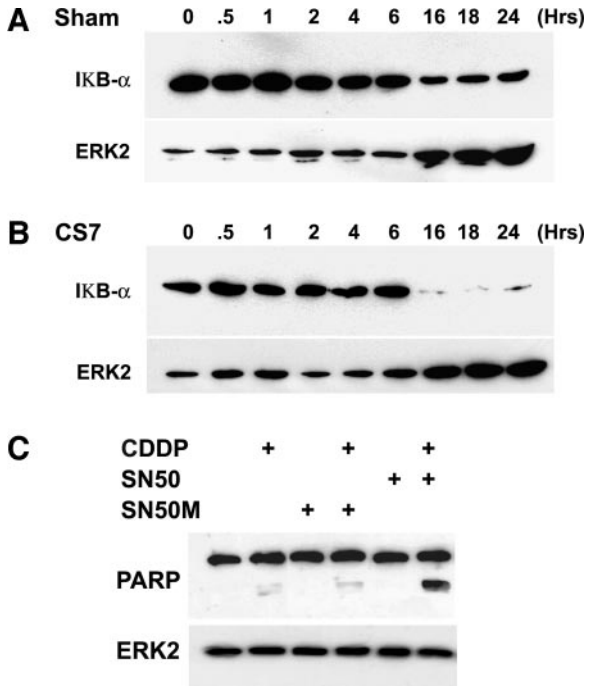

Fig. 7. CDDP effects on IκB-α protein levels and restoration of PARP cleavage. Sham cells (*A*) and a Smad7 clone (*B*) were treated for the indicated times with 50 μM CDDP. Cell lysates were subjected to immunoblotting using an IκB-a antibody. The membranes were then stripped and reprobed for ERK2 to assess protein loading. *C*, Smad7-overexpressing cells were treated for 24 h in the presence (+) or absence of 50 μM SN50 or its inactive form (SN50M) and 50 μM CDDP. Cell lysates were subjected to immunoblotting using an antibody that recognizes uncleaved and cleaved PARP.

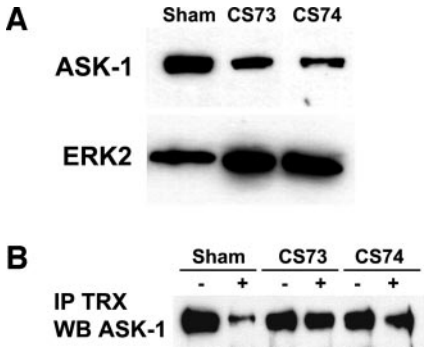

Fig. 8. Association of ASK1 with TRX. *A*, cell lysates from Sham and Smad7-overexpressing cells were subjected to immunoblotting with an anti-ASK1 antibody. The membrane was then stripped and reprobed for ERK2 to assess protein loading. *B*, Sham and Smad7-overexpressing cells were treated with CDDP and lysates immunoprecipitated for TRX. Immune complexes were subjected to immunoblotting with an anti-ASK1 antibody.

growth-inhibitory actions of TGF-βs (49, 50). Conversely, expression of oncogenic K-*ras* may confer an aggressive cancer phenotype through posttranslational modification of the type III TGF-β receptor (51). Together, these observations imply that perturbations in TGF-β-dependent signaling pathways occur frequently in human cancers.

Epidermal growth factor up-regulates the expression of Smad7 in lung cancer cell lines (52), and there is an overexpression of multiple epidermal growth factor-like ligands, the epidermal growth factor receptor, and related tyrosine kinase receptors in PDAC (53). These observations raise the possibility that excessive mitogenic signaling may block cancer cell-directed inhibitory effects of TGF-β by up-regulating Smad7 expression *in vivo* (54). Yet, the overexpression of any of the three TGF-β isoforms (55) or of TβRII correlates with decreased patient survival, and TβRII overexpression is associated with increased expression of matrix-metalloproteinase-9 and plasminogen activator inhibitor 1, or PAI-1 (56). These observations suggest that TGF-βs confer a growth advantage to pancreatic cancer cells *in vivo*. In support of this hypothesis, TGF-β1 increases the invasiveness of COLO-357 cancer cells in culture (57), whereas expression of a soluble TβRII in pancreatic cancer cells, which functions to sequester TGF-βs, leads to decreased tumor growth and metastasis in athymic nude mice (57, 58).

We have proposed previously that in pancreatic cancer cells that express high levels of Smad7, TGF-βs may act directly on the cancer cells to enhance the expression of growth-promoting genes such as *PAI-1* (14). In the present study, using the technique of differential display, we observed that COLO-357 cells that were engineered to overexpress Smad7 exhibited increased levels of TRX. The concomitant overexpression of Smad7 and TRX, at both the mRNA and protein levels, was confirmed in three different Smad7-overexpressing clones. Furthermore, using real-time PCR to analyze mRNA expression in laser-captured cancer cells, we found an extremely close correlation between Smad7 and TRX expression in PDAC samples. Therefore, in addition to its ability to inhibit TβRI-mediated phosphorylation of Smad2 and Smad3, it is likely that high levels of Smad7 may act to up-regulate TRX expression. Although the specific mechanisms by which this up-regulation is mediated are not known, it has been established that Smad7 may also function as a TGF-β-independent transcriptional modulator (5). It is possible, therefore, that Smad7 up-regulates TRX expression through a transcriptional mechanism. However, in view of the fact that the time-dependent decrease in TRX mRNA levels that was observed when COLO-357 cells and Smad7 transfected clones were incubated under serum-free conditions was attenuated by TGF-β1, it is possible that TGF-β may also act independently of Smad7 to enhance TRX mRNA half-life.

Irrespective of the mechanism of TRX up-regulation, several lines of evidence suggest that the Smad7-associated increase in TRX expression conferred a growth advantage to COLO-357 cells. First, the Smad7-associated increase in anchorage-independent growth was markedly attenuated after suppression of TRX expression with a TRX antisense construct. Second, PX-12, an inhibitor of TRX activity, greatly inhibited the anchorage-dependent growth of COLO-357 cells, and this inhibitory effect was markedly attenuated in CS7 clones that expressed high levels of TRX. Third, PX-12 enhanced the growth inhibitory actions of CDDP in Sham-transfected COLO-357 cells, and this effect was also markedly attenuated in TRX-overexpressing CS7

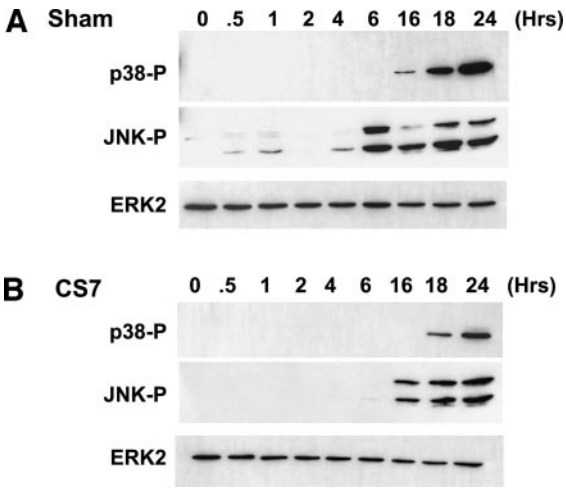

Fig. 9. Activation of p38 and JNK by CDDP. Sham (*A*) and Smad7-overexpressing (*B*) cells were treated for the indicated times with 50 μM CDDP. Cell lysates (20 μg/lane) were subjected to SDS-PAGE and probed for active p38 and JNK using the respective phosphospecific antibodies. Blots were then stripped and probed for ERK2 to assess protein loading.

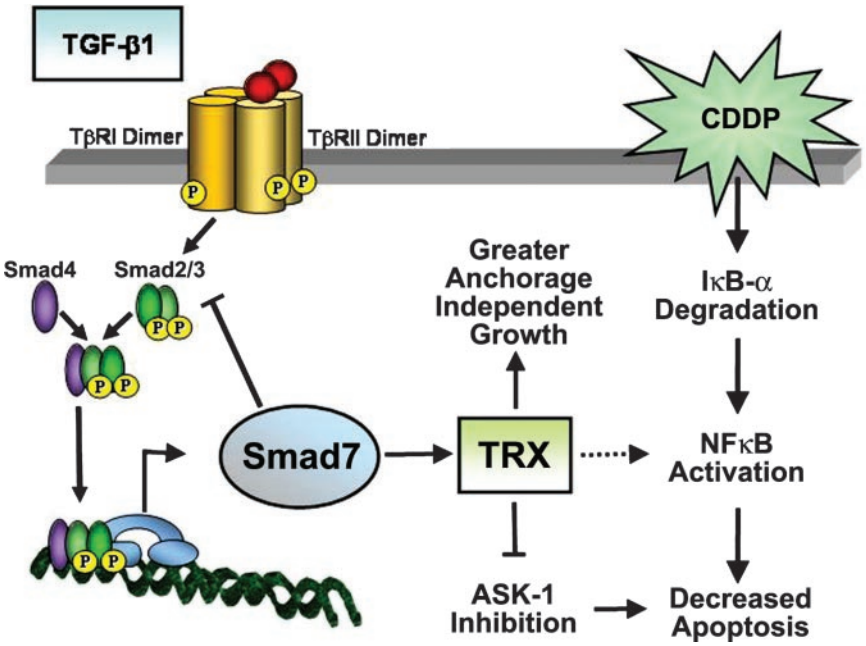

Fig. 10. Hypothetical model of TGF-β signaling in a pancreatic cancer. TGF-β1 is shown activating the TβR heterotetrameric complex, leading to activation of the classical Smad2/3/4 signaling cascade. Smad7, in addition to potentially acting as a negative regulator of TβRI and Smad2/3 activation, causes the induction of TRX. High TRX levels lead to increased anchorage-independent growth, suppression of ASK1, and activation of cysteine 62 on NFκB. In the presence of CDDP, there is enhanced degradation of IκB-α in these cells, leading to increased NFκB activation. Thus, CDDP-mediated induction of apoptosis is suppressed in Smad7-overexpressing cells as a consequence of ASK1 inhibition and NFκB activation.

cells. Taken together, these observations indicate that TRX confers a growth advantage to pancreatic cancer cells by promoting their anchorage-dependent and -independent growth.

Increased TRX expression protects cells from apoptosis induced by a variety of agents, such as dexamethasone, etoposide, doxorubicin, staurosporine, and CDDP (9). The latter drug exerts its cytotoxic effects principally through the formation of DNA-platinum adducts, which leads to cell cycle arrest and apoptosis (59). CDDP may also induce apoptosis by activating ASK1 (35). However, the potential clinical usefulness of CDDP is often limited by the acquisition of resistance to its cytotoxic actions, which may be due to its decreased uptake by the cancer cells, increased efflux from the cells, increased cellular DNA repair mechanisms, and increased levels of TRX, glutathione, or metallothionine (30, 60, 61). In the present study, a relatively high concentration of CDDP (50 μM) induced the activation of apoptosis in Sham cells. However, this effect was markedly decreased in the Smad7-overexpressing CS7 cells, as evidenced by attenuated effects of CDDP on DNA laddering, PARP cleavage, and caspase activation in these cells. It is likely that the high TRX levels in these cells contributed to this resistance, because TRX interacted more efficiently with ASK1 in CS7 cells by comparison with Sham cells, thereby suppressing its activity, leading to attenuated and delayed activation of JNK and p38 MAP kinase in the CS7 cells. In addition, ASK1 levels were lower in CS7 cells, most likely because of TRX-mediated ubiquitination and degradation of ASK1 (62).

In theory, CDDP could have activated ASK1 through the generation of ROS (36). It is unlikely, however, that this mechanism was operative in our cells or contributed to the resistance of CS7 cells to CDDP-mediated apoptosis, inasmuch as CDDP did not significantly alter ROS levels in either Sham or CS7 cells. By contrast, CDDP induced an increase in NFκB activation in CS7 cells, but not in Sham cells. CDDP has been reported previously to activate the NFκB pathway (63, 64), and NFκB activation mediates resistance to apoptosis (65). It is likely, therefore, that in addition to the differential regulation of ASK1, JNK, and p38 MAP kinase activities in CS7 by comparison with Sham cells, the activation of NFκB also contributed to the apoptosis resistance in these cells. In support of this conclusion, the NFκB inhibitor SN50, but not its mutant inactive form, restored the ability of CDDP to induce PARP cleavage in CS7 cells.

In theory, several mechanisms may explain the ability of CDDP to induce NFκB activation in CS7 cells. Thus, cysteine 62 in NFκB must be reduced by TRX for NFκB to become active (33). However, because a relatively low level of TRX is required for such disulfide reduction of proteins, it is unlikely that this was the limiting factor that prevented CDDP activation of NFκB in Sham cells. By contrast, ASK1 is a recognized inhibitor of NFκB activation, and the TRX-mediated inhibition of ASK1 could have released NFκB from this inhibitory effect. In addition, it is well established that in its inactive form, NFκB is sequestered in the cytoplasm as a consequence of its interaction with its inhibitor, IκB-α, and that NFκB is activated after the phosphorylation and proteosome-mediated degradation of IκB-α (66). In the present study, we determined that CDDP treatment of CS7 cells was associated with a marked degradation of IκB-α, and this effect was markedly attenuated in Sham cells. Taken together, these observations indicate that CDDP-dependent activation of the NFκB pro-survival pathway in CS7 cells was most likely mediated through decreased IκB-α protein levels and TRX-mediated suppression of ASK1.

PDAC is characterized by the presence of high levels of TGF-βs (55) and by parallel increases in Smad7 and TRX (present findings). TGF-βs may act in certain cancer cells in a manner that promotes cancer growth and resistance to apoptosis (67). Similarly, TRX overexpression may lead to an increased tumorigenic potential and resistance to chemotherapeutic and pro-apoptotic agents in a number of different malignancies (9). Thus, our findings that TRX is downstream of Smad7 in pancreatic cancer cells in a pathway that acts to promote growth and induce apoptosis resistance (Fig. 10) imply a novel regulatory function for this inhibitory Smad protein and raise the possibility that drugs that block TRX expression or action or that interfere with Smad7 function may ultimately have a therapeutic potential in PDAC.

REFERENCES

1. ten Dijke P, Miyazono K, Heldin CH. Signaling inputs converge on nuclear effectors in TGF-β signaling. Trends Biochem Sci 2000;25:64–70.
2. Nakao A, Afrakhte M, Moren A, et al. Identification of Smad7, a TGFβ-inducible antagonist of TGF-β signalling. Nature 1997;389:631–5.
3. Hayashi H, Abdollah S, Qiu Y, et al. The MAD-related protein Smad7 associates with the TGFβ receptor and functions as an antagonist of TGFβ signaling. Cell 1997;89:1165–73.

4. Itoh S, Landstrom M, Hermansson A, et al. Transforming growth factor β1 induces nuclear export of inhibitory Smad7. J Biol Chem 1998;273:29195–201.
5. Pulaski L, Landstrom M, Heldin CH, Souchelnytskyi S. Phosphorylation of Smad7 at Ser-249 does not interfere with its inhibitory role in transforming growth factor-β-dependent signaling but affects Smad7-dependent transcriptional activation. J Biol Chem 2001;276:14344–9.
6. Bai S, Cao X. A nuclear antagonistic mechanism of inhibitory Smads in transforming growth factor-β signaling. J Biol Chem 2002;277:4176–82.
7. Gronroos E, Hellman U, Heldin CH, Ericsson J. Control of Smad7 stability by competition between acetylation and ubiquitination. Mol Cell 2002;10:483–93.
8. Ferrigno O, Lallemand F, Verrecchia F, et al. Yes-associated protein (YAP65) interacts with Smad7 and potentiates its inhibitory activity against TGF-β/Smad signaling. Oncogene 2002;21:4879–84.
9. Powis G, Montfort WR. Properties and biological activities of thioredoxins. Annu Rev Pharmacol Toxicol 2001;41:261–95.
10. Muller JM, Rupec RA, Baeuerle PA. Study of gene regulation by NF-κB and AP-1 in response to reactive oxygen intermediates. Methods 1997;11:301–12.
11. Gallegos A, Gasdaska JR, Taylor CW, et al. Transfection with human thioredoxin increases cell proliferation and a dominant-negative mutant thioredoxin reverses the transformed phenotype of human breast cancer cells. Cancer Res 1996;56:5765–70.
12. Korc M. Biology of pancreatic cancer. In: Rustgi AK, editor. Gastrointestinal cancers. London: W. B. Saunders, Co.; 2003 p. 519–28.
13. Hahn SA, Hoque AT, Moskaluk CA, et al. Homozygous deletion map at 18q21.1 in pancreatic cancer. Cancer Res 1996;56:490–4.
14. Kleeff J, Ishiwata T, Maruyama H, et al. The TGF-β signaling inhibitor Smad7 enhances tumorigenicity in pancreatic cancer. Oncogene 1999;18:5363–72.
15. Baldwin RL, Friess H, Yokoyama M, et al. Attenuated ALK5 receptor expression in human pancreatic cancer: correlation with resistance to growth inhibition. Int J Cancer 1996;67:283–8.
16. Kleeff J, Korc M. Up-regulation of transforming growth factor (TGF)-β receptors by TGF-β1 in COLO-357 cells. J Biol Chem 1998;273:7495–500.
17. Kornmann M, Ishiwata T, Beger HG, Korc M. Fibroblast growth factor-5 stimulates mitogenic signaling and is overexpressed in human pancreatic cancer: evidence for autocrine and paracrine actions. Oncogene 1997;15:1417–24.
18. Liang P, Pardee AB. Differential display of eukaryotic messenger RNA by means of the polymerase chain reaction. Science 1992;257:967–71.
19. Kornmann M, Danenberg KD, Arber N, Beger HG, Danenberg PV, Korc M. Inhibition of cyclin D1 expression in human pancreatic cancer cells is associated with increased chemosensitivity and decreased expression of multiple chemoresistance genes. Cancer Res 1999;59:3505–11.
20. Mosmann T. Rapid colorimetric assay for cellular growth and survival: application to proliferation and cytotoxicity assays. J Immunol Methods 1983;65:55–63.
21. Raitano AB, Korc M. Tumor necrosis factor up-regulates γ-interferon binding in a human carcinoma cell line. J Biol Chem 1990;265:10466–72.
22. Friess H, Yamanaka Y, Buchler M, et al. Enhanced expression of the type II transforming growth factor β receptor in human pancreatic cancer cells without alteration of type III receptor expression. Cancer Res 1993;53:2704–7.
23. Simone NL, Bonner RF, Gillespie JW, Emmert-Buck MR, Liotta LA. Laser-capture microdissection: opening the microscopic frontier to molecular analysis. Trends Genet 1998;14:272–6.
24. Dignam JD, Lebovitz RM, Roeder RG. Accurate transcription initiation by RNA polymerase II in a soluble extract from isolated mammalian nuclei. Nucleic Acids Res 1983;11:1475–89.
25. Zhang Y, Han H, Wang J, Wang H, Yang B, Wang Z. Impairment of human ether-a-go-go-related gene (HERG) K^+ channel function by hypoglycemia and hyperglycemia: similar phenotypes but different mechanisms. J Biol Chem 2003;278:10417–26.
26. Vogt A, Tamura K, Watson S, Lazo JS. Antitumor imidazolyl disulfide IV-2 causes irreversible G(2)/M cell cycle arrest without hyperphosphorylation of cyclin-dependent kinase Cdk1. J Pharmacol Exp Ther 2000;294:1070–5.
27. Pettersson F, Colston KW, Dalgleish AG. Retinoic acid enhances the cytotoxic effects of gemcitabine and cisplatin in pancreatic adenocarcinoma cells. Pancreas 2001;23:273–9.
28. Lee JU, Hosotani R, Wada M, et al. Mechanism of apoptosis induced by cisplatin and VP-16 in PANC-1 cells. Anticancer Res 1997;17:3445–50.
29. Nordberg J, Arner ES. Reactive oxygen species, antioxidants, and the mammalian thioredoxin system. Free Radic Biol Med 2001;31:1287–312.
30. Yokomizo A, Ono M, Nanri H, et al. Cellular levels of thioredoxin associated with drug sensitivity to cisplatin, mitomycin C, doxorubicin, and etoposide. Cancer Res 1995;55:4293–6.
31. Baker A, Payne CM, Briehl MM, Powis G. Thioredoxin, a gene found overexpressed in human cancer, inhibits apoptosis in vitro and in vivo. Cancer Res 1997;57:5162–7.
32. Sasada T, Nakamura H, Ueda S, et al. Possible involvement of thioredoxin reductase as well as thioredoxin in cellular sensitivity to cis-diamminedichloroplatinum (II). Free Radic Biol Med 1999;27:504–14.
33. Nishi T, Shimizu N, Hiramoto M, et al. Spatial redox regulation of a critical cysteine residue of NF-κB in vivo. J Biol Chem 2002;277:44548–56.
34. Ichijo H, Nishida E, Irie K, et al. Induction of apoptosis by ASK1, a mammalian MAPKKK that activates SAPK/JNK and p38 signaling pathways. Science 1997;275:90–4.
35. Chen Z, Seimiya H, Naito M, et al. ASK1 mediates apoptotic cell death induced by genotoxic stress. Oncogene 1999;18:173–80.
36. Saitoh M, Nishitoh H, Fujii M, et al. Mammalian thioredoxin is a direct inhibitor of apoptosis signal-regulating kinase (ASK) 1. EMBO J 1998;17:2596–606.
37. Tobiume K, Saitoh M, Ichijo H. Activation of apoptosis signal-regulating kinase 1 by the stress-induced activating phosphorylation of pre-formed oligomer. J Cell Physiol 2002;191:95–104.
38. Bishopric NH, Webster KA. Preventing apoptosis with thioredoxin: ASK me how. Circ Res 2002;90:1237–9.
39. Derynck R, Akhurst RJ, Balmain A. TGF-β signaling in tumor suppression and cancer progression. Nat Genet 2001;29:117–29.
40. Hahn SA, Schutte M, Hoque AT, et al. DPC4, a candidate tumor suppressor gene at human chromosome 18q21.1. Science 1996;271:350–3.
41. Kleeff J, Maruyama H, Friess H, Buchler MW, Falb D, Korc M. Smad6 suppresses TGF-β-induced growth inhibition in COLO-357 pancreatic cancer cells and is overexpressed in pancreatic cancer. Biochem Biophys Res Commun 1999;255:268–73.
42. Park K, Kim SJ, Bang YJ, et al. Genetic changes in the transforming growth factor β (TGF-β) type II receptor gene in human gastric cancer cells: correlation with sensitivity to growth inhibition by TGF-β. Proc Natl Acad Sci USA 1994;91:8772–6.
43. Kim IY, Ahn HJ, Zelner DJ, Shaw JW, Sensibar JA, Kim JH, Kato M, Lee C. Genetic change in transforming growth factor β (TGF-β) receptor type I gene correlates with insensitivity to TGF-β 1 in human prostate cancer cells. Cancer Res 1996;56:44–8.
44. Wang J, Han W, Zborowska E, et al. Reduced expression of transforming growth factor β type I receptor contributes to the malignancy of human colon carcinoma cells. J Biol Chem 1996;271:17366–71.
45. Wyllie FS, Dawson T, Bond JA, et al. Correlated abnormalities of transforming growth factor-β 1 response and p53 expression in thyroid epithelial cell transformation. Mol Cell Endocrinol 1991;76:13–21.
46. Laiho M, DeCaprio JA, Ludlow JW, Livingston DM, Massague J. Growth inhibition by TGF-β linked to suppression of retinoblastoma protein phosphorylation. Cell 1990;62:175–85.
47. Filmus J, Zhao J, Buick RN. Overexpression of H-ras oncogene induces resistance to the growth-inhibitory action of transforming growth factor β-1 (TGF-β 1) and alters the number and type of TGF-β 1 receptors in rat intestinal epithelial cell clones. Oncogene 1992;7:521–6.
48. Zhao J, Buick RN. Regulation of transforming growth factor β receptors in H-ras oncogene-transformed rat intestinal epithelial cells. Cancer Res 1995;55:6181–8.
49. Hartsough MT, Mulder KM. Transforming growth factor β activation of p44mapk in proliferating cultures of epithelial cells. J Biol Chem 1995;270:7117–24.
50. Hartsough MT, Frey RS, Zipfel PA, et al. Altered transforming growth factor signaling in epithelial cells when ras activation is blocked. J Biol Chem 1996;271:22368–75.
51. Yan Z, Deng X, Friedman E. Oncogenic Ki-ras confers a more aggressive colon cancer phenotype through modification of transforming growth factor-β receptor III. J Biol Chem 2001;276:1555–63.
52. Afrakhte M, Moren A, Jossan S, et al. Induction of inhibitory Smad6 and Smad7 mRNA by TGF-β family members. Biochem Biophys Res Commun 1998;249:505–11.
53. Korc M. Role of growth factors in pancreatic cancer. Surg Oncol Clin N Am 1998;7:25–41.
54. Yamanaka Y, Friess H, Kobrin MS, Buchler M, Beger HG, Korc M. Coexpression of epidermal growth factor receptor and ligands in human pancreatic cancer is associated with enhanced tumor aggressiveness. Anticancer Res 1993;13:565–9.
55. Friess H, Yamanaka Y, Buchler M, et al. Enhanced expression of transforming growth factor β isoforms in pancreatic cancer correlates with decreased survival. Gastroenterology 1993;105:1846–56.
56. Wagner M, Kleeff J, Friess H, Buchler MW, Korc M. Enhanced expression of the type II transforming growth factor-β receptor is associated with decreased survival in human pancreatic cancer. Pancreas 1999;19:370–6.
57. Rowland-Goldsmith MA, Maruyama H, Kusama T, Ralli S, Korc M. Soluble type II transforming growth factor-β (TGF-β) receptor inhibits TGF-β signaling in COLO-357 pancreatic cancer cells in vitro and attenuates tumor formation. Clin Cancer Res 2001;7:2931–40.
58. Rowland-Goldsmith MA, Maruyama H, Matsuda K, et al. Soluble type II transforming growth factor-β receptor attenuates expression of metastasis-associated genes and suppresses pancreatic cancer cell metastasis. Mol Cancer Ther 2002;1:161–7.
59. Siddik ZH. Cisplatin: mode of cytotoxic action and molecular basis of resistance. Oncogene 2003;22:7265–79.
60. Arner ES, Nakamura H, Sasada T, Yodoi J, Holmgren A, Spyrou G. Analysis of the inhibition of mammalian thioredoxin, thioredoxin reductase, and glutaredoxin by cis-diamminedichloroplatinum (II) and its major metabolite, the glutathione-platinum complex. Free Radic Biol Med 2001;31:1170–8.
61. Kawahara N, Tanaka T, Yokomizo A, et al. Enhanced coexpression of thioredoxin and high mobility group protein 1 genes in human hepatocellular carcinoma and the possible association with decreased sensitivity to cisplatin. Cancer Res 1996;56:5330–3.
62. Liu Y, Min W. Thioredoxin promotes ASK1 ubiquitination and degradation to inhibit ASK1-mediated apoptosis in a redox activity-independent manner. Circ Res 2002;90:1259–66.
63. Sodhi A, Singh RA. Mechanism of NF-κ B translocation in macrophages treated in vitro with cisplatin. Immunol Lett 1998;63:9–17.
64. Yeh PY, Chuang SE, Yeh KH, Song YC, Ea CK, Cheng AL. Increase of the resistance of human cervical carcinoma cells to cisplatin by inhibition of the MEK to ERK signaling pathway partly via enhancement of anticancer drug-induced NF κB activation. Biochem Pharmacol 2002;63:1423–30.
65. Karin M, Cao Y, Greten FR, Li ZW. NF-κB in cancer: from innocent bystander to major culprit. Nature Rev Cancer 2002;2:301–10.
66. Bharti AC, Aggarwal BB. Nuclear factor-κB and cancer: its role in prevention and therapy. Biochem Pharmacol 2002;64:883–8.
67. Wakefield LM, Roberts AB. TGF-β signaling: positive and negative effects on tumorigenesis. Curr Opin Genet Dev 2002;12:22–9.

Thioredoxin Is Downstream of Smad7 in a Pathway That Promotes Growth and Suppresses Cisplatin-Induced Apoptosis in Pancreatic Cancer

Nichole Boyer Arnold, Knut Ketterer, Jörg Kleeff, et al.

Cancer Res 2004;64:3599-3606.